Compensatory Mutations in Predicted Metal Transporters Modulate Auxin Conjugate Responsiveness in *Arabidopsis*

Rebekah A. Rampey,* Megan T. Baldridge,[†,1] David C. Farrow,*[,2] Sarah N. Bay,*[,3] and Bonnie Bartel[†,4]
*Department of Biology, Harding University, Searcy, Arkansas 72149, and [†]Department of Biochemistry and Cell Biology, Rice University, Houston, Texas 77005

ABSTRACT Levels of the phytohormone indole-3-acetic acid (IAA) can be altered by the formation and hydrolysis of IAA conjugates. The isolation and characterization of *Arabidopsis thaliana* mutants with reduced IAA-conjugate sensitivity and wild-type IAA responses is advancing the understanding of auxin homeostasis by uncovering the factors needed for conjugate metabolism. For example, the discovery that the IAA-Ala-resistant mutant *iar1* is defective in a protein in the ZIP family of metal transporters uncovered a link between metal homeostasis and IAA-conjugate sensitivity. To uncover additional factors impacting auxin conjugate metabolism, we conducted a genetic modifier screen and isolated extragenic mutations that restored IAA-amino acid conjugate sensitivity to the *iar1* mutant. One of these suppressor mutants is defective in a putative cation diffusion facilitator, MTP5 (At3g12100; formerly known as MTPc2). Loss of MTP5 function restored IAA conjugate sensitivity to *iar1* but not to mutants defective in IAA-amino acid conjugate amidohydrolases. Our results are consistent with a model in which MTP5 and IAR1 transport metals in an antagonistic fashion to regulate metal homeostasis within the subcellular compartment in which the IAA-conjugate amidohydrolases reside, and support previous suggestions that the ion composition in this compartment influences hydrolase activity.

Certain trace elements are essential for plant growth and development. For example, Cu^{2+} and Mn^{2+} are used in many electron transfer reactions, including those in photosynthesis, Zn^{2+} ions provide structure to DNA-binding proteins and serve as cofactors for hydrolytic enzymes, and iron is essential for heme proteins such as ferredoxin and catalase [reviewed in (Clemens *et al.* 2002; Hall and Williams 2003)]. When appropriate levels of any of these ions are not main-

tained, plants display an array of symptoms, including reduced growth (Marschner 1995).

Numerous cation transporters facilitate ion homeostasis. In *Arabidopsis*, there are at least 880 putative membrane transporters that fall into 46 families (Mäser *et al.* 2001). Disruption of some of these transporters leads to measurable metal-related phenotypes in single mutants (Cheng *et al.* 2003; Delhaize *et al.* 2007; Li *et al.* 2008; Kawachi *et al.* 2009). However, not all mutants defective in putative metal transporters display morphological or ionomic phenotypes due to the complexity and redundancy of the elaborate metal transport system. Establishing function for some of these predicted transporters may require alternative genetic, biochemical, or physiological analyses.

Auxin is a plant hormone that controls a plethora of growth and developmental processes, and auxin metabolism is complex and distributed among several subcellular compartments (Woodward and Bartel 2005; Strader and Bartel 2011). By screening for *Arabidopsis* mutants with defective indole-3-acetic acid (IAA) conjugate responsiveness, we uncovered several enzymes that hydrolyze conjugates (Bartel and Fink 1995; Davies *et al.* 1999; Rampey *et al.* 2004). These IAA-amino acid hydrolases contain predicted N-terminal signal sequences and C-terminal endoplasmic reticulum (ER) retention signals (Bartel and Fink 1995; Davies *et al.* 1999), and several localize to

[1]Present address: Department of Pathology & Immunology, Washington University School of Medicine, St. Louis, MO 63110.
[2]Present address: Department of Computational Biology, Carnegie Mellon University, Pittsburgh, PA 15213.
[3]Present address: Department of Human Genetics, Emory University, Atlanta, GA 30322.
[4]Corresponding author: Department of Biochemistry and Cell Biology, MS-140, Rice University, 6100 S. Main St., Houston, TX 77005. E-mail: bartel@rice.edu

the ER in organelle proteomics experiments (Dunkley et al. 2006). The observation that the IAA-amino acid hydrolases are metalloenzymes (Bartel and Fink 1995; Davies et al. 1999; Rampey et al. 2004; Bitto et al. 2009) may explain why proteins that are likely to influence metal transport also have emerged from screens for reduced IAA-conjugate responsiveness. Analyses of the IAA-conjugate response mutants iaa-leucine resistant2 (ilr2) (Magidin et al. 2003), ilr3 (Rampey et al. 2006), and iaa-alanine resistant1 (iar1) (Lasswell et al. 2000) reveal a critical role for the metal microenvironment in IAA-conjugate metabolism and indicate that an understanding of subcellular metal homeostasis will be required to fully elucidate mechanisms regulating IAA levels. For example, ilr2 seedlings are resistant to root growth inhibition not only by IAA conjugates but also by Mn^{2+} and Co^{2+} (Magidin et al. 2003). ILR2 (At3g18485) is an apparently cytosolic protein that may inhibit an unidentified metal transporter, as ilr2 microsomes have enhanced Mn^{2+} transport activity compared with wild-type microsomes (Magidin et al. 2003). In addition, the ILR3 (At5g54680) basic helix–loop–helix leucine zipper (bHLH105) transcription factor regulates transcription of metal transporter genes (Rampey et al. 2006) that appear to modulate iron distribution (Gollhofer et al. 2011). A dominant gain-of-function ilr3 allele reduces IAA-Leu and Mn^{2+} responsiveness, whereas loss of ILR3 heightens responses to both IAA-Leu and Mn^{2+} (Rampey et al. 2006).

The iar1 mutant has decreased sensitivity to a variety of IAA conjugates (Lasswell et al. 2000) that are in vitro substrates of the Arabidopsis IAA-amino acid hydrolases (LeClere et al. 2002). IAR1 (At1g68100) contains at least seven predicted transmembrane domains and many His-rich regions, consistent with a role in metal binding or transport (Lasswell et al. 2000). IAR1 resembles members of the zinc-regulated transporter iron-regulated transporter-like protein (ZIP) family that transport metals from the vacuole or apoplast into the cytosol (Gaither and Eide 2000). Although there are at least 15 ZIP family members in Arabidopsis (Hall and Williams 2003), IAR1 is the only Arabidopsis member of the LIV-1 zinc transporter (LZT) subfamily (Taylor and Nicholson 2003). Heterologous expression of mouse LZT protein ZIP7/KE4, which is 26% identical to IAR1, complements the Arabidopsis iar1 mutant (Lasswell et al. 2000) and the Saccharomyces cerevisiae yke4 mutant (Kumánovics et al. 2006), suggesting that IAR1, ZIP7, and YKE4 are orthologs that function similarly in plants, animals, and yeast. Although the localization and substrate specificity of Arabidopsis IAR1 have not been determined, mammalian ZIP7/KE4 is a zinc exporter localized in the Golgi membrane (Huang et al. 2005), and yeast Yke4p is a bidirectional zinc transporter localized in the ER membrane (Kumánovics et al. 2006), consistent with the possibility that IAR1 is a zinc transporter in the secretory pathway. Determining the function of IAR1 may provide insight into IAA-conjugate responses and metabolism in plants and contribute to understanding the function of other members of the LZT transporter family.

The observation the IAA-conjugate hydrolases require metal cofactors for activity (Bartel and Fink 1995; Davies et al. 1999; Rampey et al. 2004) underlies the hypothesis that the direct consequences of ilr2, ilr3, and iar1 mutations are alterations in ion homeostasis, and the altered sensitivity to IAA conjugates in these mutants is a secondary effect of this change. Indeed, exogenous manganese suppresses the IAA-Ala resistance of iar1 (Lasswell et al. 2000), and ion level alterations are detected in ilr3 mutants grown on certain media (Rampey et al. 2006). However, ionomic changes have not been identified in either ilr2 (Magidin et al. 2003) or iar1 (Lasswell et al. 2000) plants, and iar1 mutants lack morphological phenotypes expected from a dra-

matic ion imbalance, suggesting that any such ionomic changes are modest or restricted to specific tissues or subcellular locations.

We have taken a genetic approach to clarify the role of IAR1 in IAA-conjugate sensitivity. We conducted an iar1 suppressor screen to isolate genes that when defective restore wild-type IAA-conjugate sensitivity to iar1 roots. We identified mtp5 as a mutant defective in a cation diffusion facilitator family transporter that suppressed the IAA-conjugate resistance of iar1 but not other IAA-conjugate sensitivity mutants. The isolation of mtp5 as an iar1 suppressor supports the hypothesis that IAR1 functions as a metal transporter and suggests that MTP5 and IAR1 transport ions in an antagonistic fashion to control subcellular metal homeostasis.

MATERIALS AND METHODS

Plant materials and growth conditions

Plants from the Columbia (Col-0) and Wassilewskija (Ws) accessions were used. For phenotypic assays, seeds were surface-sterilized (Last and Fink 1988) and grown aseptically on plant nutrient medium containing 0.5% (w/v) sucrose [PNS (Haughn and Somerville 1986)] solidified with 0.6% agar. Seedlings were grown in medium alone or medium supplemented with IAA, IAA-L-amino acid conjugates (Sigma-Aldrich) or other hormones (from 0.1, 1, or 100 mM stocks in ethanol), or Basta [glufosinate ammonium, Crescent Chemical, Augsburg, Germany; from a 50 mg/mL stock in 25% (v/v) ethanol]. Media supplemented with metals (from 100 mM $MnCl_2$, 500 mM $CoCl_2$, 2 M $CaCl_2$, 20 mM $CdCl_2$, and 500 mM $ZnSO_4$ stocks in H_2O) were prepared without sucrose. Plates were sealed with gas-permeable Leukopor surgical tape (LecTec Corp, Minnetonka, MN) and incubated with constant illumination (25 to 45 $\mu Em^{-2}s^{-2}$) at 22° under yellow long-pass filters to slow the breakdown of indolic compounds (Stasinopoulos and Hangarter 1990). Plants transferred to soil (Metromix 200, Scotts, Marysville, OH) were grown at 22 to 25° under continuous illumination by Cool White fluorescent bulbs (Sylvania, Danvers, MA).

Mutant isolation

Approximately 48,000 progeny of iar1-3 (Col-0 accession) mutagenized with ethyl methanesulfonate (Normanly et al. 1997) and iar1-1 (Ws accession) mutagenized with fast-neutron bombardment (Lasswell 2000) were screened for iar1 suppressors by plating ~1000 seeds per 150 mm plate on PNS supplemented with 40 μM IAA-Ala. Seedlings were screened after growing for 8 d in continuous yellow-filtered light at 22°. Seedlings with wild-type sensitivity to IAA-Ala were transferred to PNS and allowed to recover, and seedlings with roots that failed to elongate after transfer were discarded. The remaining mutants were transferred to soil for seed production. Progeny of these plants were tested on 40 μM IAA-Ala and PNS. Homozygous iar1 mutations in the suppressors were confirmed using polymerase chain reaction (PCR) amplification and restriction analyses. The iar1-1 mutation was detected as described previously (Lasswell et al. 2000), and the iar1-3 mutation was detected by PCR amplification with the oligonucleotides 5′-GAACCAGGA-CAATCATCGTTG-3′ and 5′-CCCAAGCTTGGGATTTCTATA-TCGGTTAC-3′ followed by digestion of the resulting product with HaeIII to yield a 328-bp product for Col-0 and 258-bp and 70-bp products for iar1-3.

The mtp5-1 mutant was isolated as suppressor of iar1-3, a loss-of-function iar1 allele in the Col-0 accession (Lasswell et al. 2000). To maintain iar1 in the mapping population, the N13 (mtp5-1 iar1-3) isolate was outcrossed to iar1-1 [in the Ws accession (Lasswell et al. 2000)]. The F_2 progeny from this outcross were plated on 40 μM

IAA-Ala, and seedlings displaying wild-type root lengths were selected for PCR-based recombination mapping. The causative mutation was located to the top of chromosome 3 using the published markers nga172 and nga162 (Bell and Ecker 1994). To further delineate the mapping interval, new PCR-based markers were designed (Table 1).

A candidate gene within the mapping region, *At3g12100*, was PCR-amplified and sequenced using DNA from an N13 mapping plant with the following oligonucleotides: T21B14-7 (5′-ATAAAGAATACAACTTTTTCTAGCTTTTAG-3′) and T21B14-9 (5′-TGAATAAAAGTGTCTTCTTGCTTGACTACA-3′), T21B14-13 (5′-GGAAATATGTACACATTCGAGGAACGATT-3′) and T21B14-17 (5′-CTTTGATTTGTTTAATATTTGACATATGTG-3′), T21B14-18 (5′-TATGAGCATCAATTCATACAAGTCTAAACA-3′) and T21B14-19 (5′-ATCGGCAGATGAAGAGACTGTTTCTGCTAA-3′), and T21B14-20 (5′-ATCAGGCTTCTTCCTTGAAGTTGCCATTGCA-3′) and T21B14-21 (5′-TTGGTAACGTAACTGTAAATCTTCTCT-3′). A G-to-A mutation was found in the 3′-splice site preceding exon 8 at nucleotide 2003 (where 1 is the A in the initiator ATG).

The *mtp5-2* mutant is a sequence-indexed *Arabidopsis* T-DNA insertion mutant (GABI_351G01) isolated by the GABI-Kat facility (Rosso *et al.* 2003). We verified the position of the T-DNA insert in *mtp5-2* by using PCR amplification with the oligonucleotides MTPc2-12 (5′-TGTAGTCAAGCAAGAAGACACTTTTATTCA-3′) and MTPc2-13 (5′-TATGCTGCAGCCTACAGAAAAGCAGAAGAT-3′) and the T-DNA specific primer, LB1-GABI (5′-CTTTCTTTTTTCCATATTGACCATCA-3′). PCR amplification of MTPc2-12 and MTPc2-13 yielded a 309 bp product from wild-type genomic DNA, whereas amplification with MTPc2-13 and LB1-GABI yielded a 250-bp product from *mtp5-2* genomic DNA. This product was sequenced, revealing that the T-DNA insertion is located in exon 7 at position *1873* in *MTP5* (where 1 is the A in the initiator ATG).

ilr1-5 is a missense mutation the Col-0 accession (Rampey *et al.* 2006) that was backcrossed to Col-0 five times prior to crossing with

mtp5-1. *iar3-1* is a missense mutation in the Ws accession (Davies *et al.* 1999) that was introgressed into Col-0 by three rounds of outcrossing prior to crossing with *mtp5-1*. *mtp5-1 ilr1-5* and *mtp5-1 iar3-1* double mutants were isolated from segregating F₂ populations using PCR amplification and restriction digest analyses. The *ilr1-5* mutation was followed via amplification with 4G12-43 (5′-CAATCATCGCTTCCGCTAC-3′) and 4G12-34 (5′-CCACGCAGCTACACCGCAC-3′) and digestion with *Rsa*I, resulting in 299- and 275-bp products for *ILR1* DNA and a 574-bp product for *ilr1-5* DNA. Homozygous *mtp5-1* and *iar3-1* plants were identified by following derived cleaved amplified polymorphic sequences (Michaels and Amasino 1998; Neff *et al.* 1998). Amplification with MTPc2-1 (5′-CCTAAACATAGGACCTCTGCATTTTCAAGC-3′) and MTPc2-2 (5′-TGCATCAAACTTATATACAGTCAACATGAA-3′) yields a 219-bp product. The altered nucleotide in MTPc2-1 (underlined) creates a *Hin*DIII restriction site in the *mtp5-1* product to give 189- and 30-bp products after digestion, whereas the *MTP5* product is not cleaved by *Hin*DIII. The *iar3-1* mutation was followed by amplification with ILL4-22 (5′-CCTGTGAGTCTAAAGGATCTGCCTCTCGTG-3′) and ILL4-24 (5′-CAAATCAATTGGCATTAGGTCAAGTAAGCT-3′). ILL4-24 creates a *Hin*DIII site (underlined nucleotide) in the *iar3-1* PCR product resulting in 174- and 30-bp products after digestion, whereas the 200 bp *IAR3* product remains uncut.

MTP5 cDNA isolation

To isolate a *MTP5* cDNA, RNA was isolated with RNeasy Mini Kits (QIAGEN, Valencia, CA) from 7-d-old Col-0 seedlings grown on filter paper in 150-mm plates containing PNS at 22° in yellow-filtered light. Reverse transcriptase (RT) reactions used RETROScript (Ambion, Austin, TX) on the Col-0 RNA primed with the oligonucleotide MTPc2-4 (5′-TTGCGGCCGCACCATGATCTCTAGTATACATCC-3′). The resulting cDNA was PCR-amplified using *Pfu* Turbo DNA polymerase (Stratagene) and the oligonucleotides MTPc2-4 and MTPc2-3 (5′-TCGGATCCTCGACGAAGTTGGAACTTTAAGATC-3′).

■ **Table 1 New markers used in the positional cloning of *MTP5***

Marker[a]	Oligonucleotides (5′ to 3′)	Enzyme	Size of Product, bp
F13M14-3+4	F13M14-3[b] CTTCTTCTATATTGAGTAGGTAGATTAAAA	*Bsa*BI	Col – 226
	F13M14-4 ATTACCTAAAGACTCTGATTTTATACTCTC		Ws – 196, 30
T7M13-3+4	T7M13-3 AGTTAACCAACGATAACAAGCAGATTCGTT	*Bcl*I	Col – 130, 20
	T7M13-4 CTCCTACAATCCTCTAAGAATCCATTGATC		Ws – 150
F24K9-7+8	F24K9-7 AATTTAAAATTATATGCAAACTAATTAGAT	*Bgl*II	Col – 200 + 30
	F24K9-8 GTAGCTAAAAAGTTGCTGCAAGCAAGGAAA		Ws – 230
F26K24-9+6	F26K24-6 GATAATAACGAAGAGTATGAAGTAAAAGTA	*Hpy*CHIV	Col – 523
	F26K24-9 AGATTCGATTACACTAGGCAATTTGTTATGA		Ws – 128, 395
MEC18-7+8	MEC18-7 TTCGATTCAAGACAAAGTTTAAAGTTACAA	*Bsp*HI	Col – 220
	MEC18-8[b] AATACTTTAAGTTTTGGATGTAAGATTCAT		Ws – 190, 30
F28J15-3+4	F28J15-3 AATATCGGCCAACAGTAAGTT	*Hin*P1I	Col – 400, 200
	F28J15-4 CATCACGTAACTGAGATTCC		Ws – 600
T2E22-9+10	T2E22-9[b] AGCCCTATGCACACACATGTAAAAATGGGA	*Fok*I	Col – 213
	T2E22-10 ATTCACTGATTTATTTGTTACCTAGCTAAA		Ws – 172, 41
MBK21-10+11	MBK21-10 GATACTCAAGTAGTTATCTGTTACCTTTAG	*Hinc*II	Col – 350, 150
	MBK21-11 CTAAACCATTATGTGTAATGTGTGAATTAG		Ws – 500
MGH6-2+3	MGH6-2 TAGTTTCTCTGATTACTTGTGTAGATGTGA	*Mbo*II	Col – 357
	MGH6-3[b] TATAGCTGTTCCAAGACTATAACACCGGAA		Ws – 327, 30
MRP15-3+4	MRP15-3 GTTAGAATTGGAATTAACAAGTATTACTAG	*Taq*I	Col – 251, 56
	MRP15-4 CTTGATAGCATTGGGAGCAAGCAACGAACC		Ws – 213, 56, 41

Col-0, Columbia; dCAPS, derived cleaved amplified polymorphic sequences; PCR, polymerase chain reaction; Ws, Wassilewskija.
[a] Markers reveal polymorphisms between Col-0 and Ws accessions when cut with the indicated restriction enzymes after PCR amplification with the indicated oligonucleotides.
[b] This is a dCAPS oligonucleotide (Michaels and Amasino 1998; Neff *et al.* 1998); the underlined nucleotide differs from wild-type sequence to create a restriction site in either the Col-0 or Ws PCR product.

Underlined base pairs in MTPc2-3 and MTPc2-4 were altered to create a *Sal*I or *Not*I restriction site, respectively, for subsequent subcloning. The *MTP5* RT-PCR product was cloned into the pCR4Blunt-TOPO vector (Invitrogen, Carlsbad, CA) and transformed into TOP10 *Escherichia coli* (Invitrogen, Carlsbad, CA). Sequence analysis of the TOPO-MTP5 plasmid showed that the *MTP5* sequence was mis-spliced (5′ of the *mtp5-1* mutation) compared to annotation by The *Arabidopsis* Information Resource (TAIR; www.arabidopsis.org). Sequence analysis of the RT-PCR product revealed not only the cloned mis-spliced cDNA, designated *MTP5-B*, but also a second product that matched the predicted *MTP5* sequence, designated *MTP5-A*.

Using this sequence information, *MTP5-B* was excised from pCR4Blunt-TOPO with *Eco*RI and ligated into pBluescript KS (+) (Stratagene) cut with *Eco*RI to obtain pKS-MTP5premut. *MTP5-B* is oriented in the opposite orientation as LacZ in pKS-MTP5premut. Site-directed oligonucleotide-mutagenesis (Ausubel *et al.* 1999) was performed using MTPc2-10 (5′-TTTACTCCGTTGATGGAA<u>G</u>T GATGTGTTTTTCGG-3′) and MTPc2-11 (5′-ATCTGCTTTCACTA ATGCTCTGTTCCTTATGTTCAT-3′) on pKS-MTP5premut. The underlined base pair in MTPc2-10 was altered to change the A to a G at nucleotide 226 (where 1 is the A in the initiator ATG of the cDNA), which caused an amino acid change from Asn to Ser. MTPc2-11 removed four nucleotides (ACAG) after nucleotide 563 in the cDNA, which changed the splicing pattern into that identified for *MTP5-A*. The mutagenized cDNA, pKS-MTP5, was identified by PCR amplification and restriction analyses. The *MTP5* coding sequence was amplified with T21B14-20 + MTPc2-7. *MTP5-B*, but not *MTP5-A*, contains a G at position 226, so the resulting product was digested with *Tsp*RI, which cleaves *MTP5-B* sequence but not *MTP5-A*. In addition, the PCR product resulting from amplification with T21B14-19 and MTPc2-9 was digested with *Pvu*II, because this site was destroyed when the 4 nucleotides were removed.

MTP5 overexpression in plants

The *MTP5* cDNA was excised from pKS-MTP5 with *Sal*I and *Not*I, restriction sites incorporated at the cDNA ends during the initial RT-PCR amplification, and was ligated into the 35S-pBARN expression vector (LeClere and Bartel 2001) cut with *Xho*I and *Not*I. The resultant pBARN-MTP5 plasmid was electroporated (Ausubel *et al.* 1999) into *Agrobacterium* GV3101 cells (Koncz *et al.* 1992) and transformed into Col-0 and *mtp5-1 iar1-3* plants using the floral dip method (Clough and Bent 1998). Transformants were selected on PN containing 10 μg/mL Basta, and homozygous lines were selected by following Basta resistance in subsequent generations.

RT-PCR analysis

RT-PCR analysis to identify the *mtp5-1* mutant coding sequence was conducted using RNA from leaves of a homozygous *mtp5-1 iar1-3* (N13) backcrossed plant as described previously. Sequencing the RT-PCR product with oligonucleotides used for amplification showed that the *mtp5-1* mutation shifts the splice site 1 bp 3′ of the original site. This shift causes a frameshift of the coding sequence that results in a stop codon after 33 bp.

To distinguish between *MTP5-A* and *MTP5-B*, we reverse transcribed the two transcripts were as described previously by using DNaseI-treated (Amplification Grade, Roche Applied Science, Indianapolis, IN) RNA from Col-0 7-d-old seedlings and the oligonucleotide MTPc2RT-1 (5′-TTCATCTTGTATAAATGCATGAAGAGCTT-3′). cDNAs were amplified with MTPc2RT-2 (5′-GTGTTGTATTCTA-CAACAGAGCTCTCTAT-3′) and MTPc2RT-1, and the resulting

products were digested with *Pvu*II to give a 312-bp product for *MTP5-A* and 246- and 66-bp products for *MTP5-B*.

RT-PCR analysis also was completed to determine whether *mtp5-2* expresses any intact *MTP5* mRNA. RNA was isolated from *mtp5-1*, *mtp5-2*, and Col-0 7-d-old seedlings as described previously and RT was performed using MTPc2-RT-4 (5′-CCATCTGAAGCAAGACA CCACCAGTGGCTT-3′) and the resulting cDNA was amplified using MTPc2-RT-3 (5′-CGTTTGCTTGCACGTCATATCAGATTCCAT-3′) and MTPc2-RT-4 to yield several splicing products spanning the *mtp5* mutations. Products detected were unspliced (404 bp), fully spliced (180 bp), intron 6 present (312 bp), and intron 7 (274 bp).

MTP5 yeast expression

The *MTP5-A* cDNA was excised from pKS-*MTP5* with *Bam*HI and *Not*I and ligated into *Bam*HI/*Not*I-cut-pTGPD, a yeast expression vector that contains the glyceraldehyde-3-phosphate dehydrogenase constitutive promoter and the *TRP1* biosynthetic gene as a selectable marker (Chang and Lindquist 1994). The resulting plasmid, pTGPD-MTP5, was sequenced with the oligonucleotides MTPc2-3 and T21B14-19 to verify the orientation of the *MTP5* cDNA.

To test whether *MTP5* could complement yeast metal transport mutants, pTGPD-MTP5 or the empty pTGPD vector were transformed (Gietz and Schiestl 1995) into cm100 (wild type), cm102 (*zrc1*), cm103 (*cot1*), and cm104 (*zrc1 cot1*) yeast strains (Eide *et al.* 1996). Transformations were plated on selective media (Ausubel *et al.* 1999) lacking Trp for cm100, lacking Trp and His for cm102, lacking Trp and Ura for cm103, and lacking Trp, His, and Ura for cm104. For metal response analysis, positive transformants were streaked on YPD (Ausubel *et al.* 1999) plates with no metals or containing $ZnSO_4$ or $CoCl_2$ and incubated at 30° for 3 d.

RESULTS

Isolation of a mutant defective in the cation diffusion facilitator MTP5

The *iar1* mutant displays reduced root elongation inhibition on several IAA-amino acid conjugates, including IAA-Ala (Lasswell *et al.* 2000). To identify genes acting with *IAR1* to control conjugate sensitivity, we conducted a genetic modifier screen to isolate extragenic mutations that suppressed the *iar1* mutant phenotype. We screened approximately 48,000 progeny of mutagenized *iar1* seeds for restored sensitivity to 40 μM IAA-Ala and isolated 61 putative suppressors, of which seven set seeds and retained wild-type IAA-Ala sensitivity in the next generation. One of these suppressors was selected for further analysis.

We used PCR-based markers to map the suppressor mutation to the top of chromosome three between nga172 and nga162 (Figure 1A, Bell and Ecker 1994). After identifying new molecular markers within this interval (Table 1), we narrowed the mapping region to ~160 kb between the markers F26K24-9+6 and F28J15-3+4 (Figure 1A). Using a candidate gene sequencing approach, we identified a mutation in the *iar1* suppressor mutant in the gene encoding a putative cation diffusion facilitator/<u>m</u>etal <u>t</u>ransport <u>p</u>rotein, MTP5 (At3g12100; Figure 1B). The *mtp5-1* mutation is a G-to-A change at nucleotide 2003 (where 1 is the A in the initiator ATG) in the 3′ splice site preceding exon 8 (Figure 1C). We sequenced *MTP5* in our other *iar1* suppressors and did not recover any additional *mtp5* alleles.

To determine the molecular consequences of the *mtp5-1* mutation, we isolated RNA from *mtp5-1* plants and reverse-transcribed and PCR-amplified the *mtp5-1* locus. Sequencing the RT-PCR product revealed that the *mtp5-1* coding sequence is spliced 1 nucleotide after
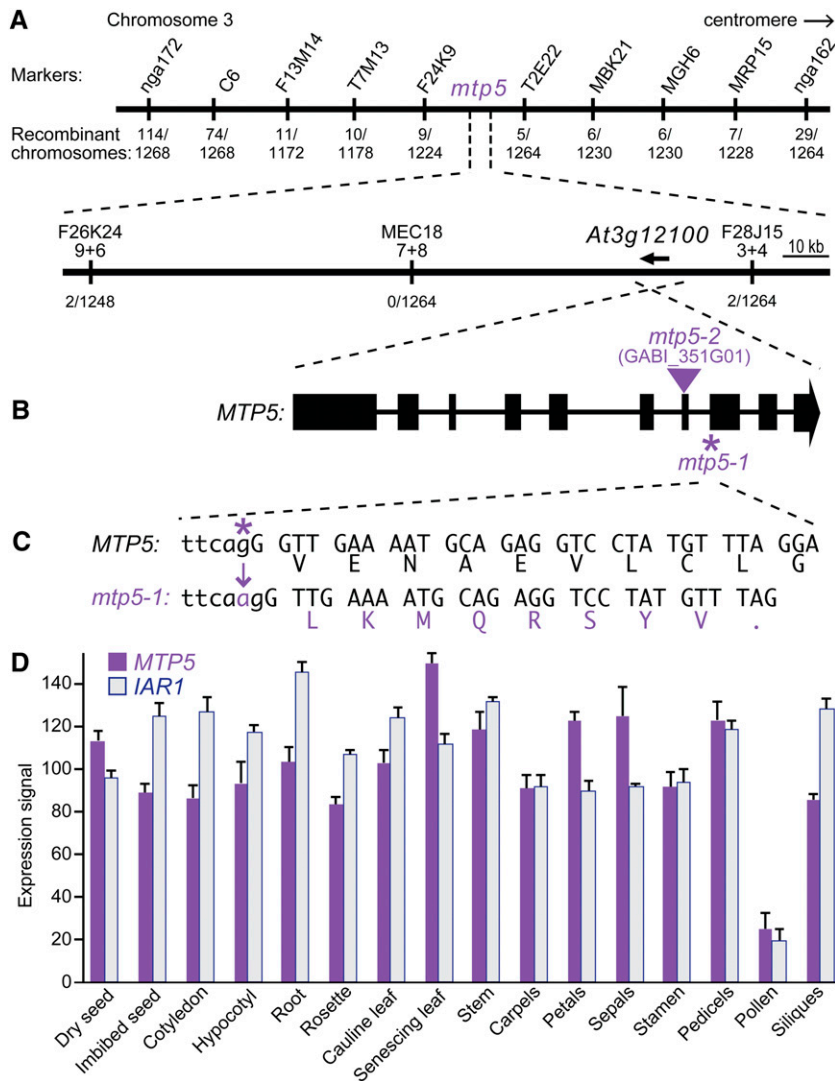
Figure 1 Positional cloning of the gene defective in *mtp5-1*. (A) Recombination mapping of *mtp5-1*. The lesion suppressing *iar1* IAA-Ala resistance was mapped to chromosome 3 between markers F26K24-9+6 and F28J15-3+4 (Table 1), an interval that includes the *MTP5* (*At3g12100*) gene. (B) *MTP5* contains 10 exons (boxes) separated by 9 introns (lines). The location of the *mtp5-2* T-DNA insertion is indicated by the triangle. (C) The G-to-A mutation in *mtp5-1* is located at position 2003 (where 1 is the A in the initiator ATG) and alters the 3′ splice site of the 7th intron (lower-case letters are intronic bases; capital letters are exonic base pairs). RT-PCR analysis revealed that the 3′ splice site in the *mtp5-1* mutant occurs 1 bp 3′ of the wild-type site, resulting in a frameshift and a premature termination codon. (D) Relative expression levels of *MTP5* and *IAR1* mRNAs in selected Arabidopsis tissues. Compiled microarray data were retrieved from the Arabidopsis eFP Browser (http://bar.utoronto.ca/efp/) in October 2012. Tissues queried were dry and imbibed (24 hr) seeds; cotyledons and hypocotyls from 7-d-old seedlings; roots from 17-d-old seedlings; vegetative rosettes from 14-d-old plants; cauline leaves from 21-d-old plants; senescing leaves from 35-d-old plants; stems from 21-d-old plants; carpels, petals, sepals, stamen, and pedicels from stage 15 flowers; mature pollen; and stage 3 siliques. Error bars show SD of mean expression signals scaled to a target intensity value of 100 for each gene.

wild type, creating a frameshift and a premature stop codon nine codons after the splicing mutation (Figure 1C). The mtp5-1 protein, if stable, would thus only encode five of the six conserved transmembrane domains (Figure 2), presumably precluding transport function.

To determine whether *MTP5* was expressed in similar tissues as *IAR1*, we examined publicly available microarray datasets (Winter *et al.* 2007). We found that *MTP5*, like *IAR1*, was widely present at similar levels across many tissues (Figure 1D), consistent with the possibility that the MTP5 and IAR1 proteins might influence similar functions.

mtp5 restores IAA-conjugate sensitivity to iar1

iar1 mutants are resistant to a variety of IAA-amino acid conjugates, including IAA-Ala, IAA-Leu, and IAA-Phe (Lasswell *et al.* 2000). We found that the *mtp5-1* mutation was recessive (data not shown) and restored *iar1* root sensitivity not only to IAA-Ala, which we used to isolate the mutant, but also to IAA-Leu and IAA-Phe (Figure 3A). This suppression did not result from generalized auxin resistance because *iar1-3 mtp5-1* seedling roots retained wild-type sensitivity to the inhibitory effects of IAA on root elongation (Figure 3B). Beyond restored IAA-amino acid conjugate sensitivity, *iar1-3 mtp5-1* seedlings did not exhibit obvious morphological abnormalities and displayed wild-type numbers of lateral roots and normal hypocotyl lengths (data not shown).

Interestingly, when the *mtp5-1* mutation was removed from the *iar1* mutant background, *mtp5-1 IAR1* seedlings were slightly more sensitive to root elongation inhibition by IAA conjugates than wild-type seedlings (Figure 3A). The single mutant was not more sensitive to free IAA (Figure 3B), however, again indicating that MTP5 specifically dampens responsiveness to IAA-amino acid conjugates.

Alternative splicing of MTP5 transcripts

We obtained a second *mtp5* allele, designated *mtp5-2*, from the GABI-Kat collection of sequence-indexed T-DNA insertion mutants (Rosso *et al.* 2003). Sequencing the insertion site revealed that the T-DNA was inserted in the seventh *MTP5* exon (Figure 4A) near the site of the *mtp5-1* lesion (Figure 2), and RT-PCR analysis confirmed that the *mtp5-2* allele lacked intact *MTP5* RNA (Figure 4B).

In the course of analyzing *mtp5-2* RNA, we found that the *MTP5* introns 6 and 7 were inefficiently spliced in both wild-type and *mtp5-1* seedlings. In addition to fully spliced product, we detected partially processed *MTP5* mRNA (Figure 4B). Interestingly, the partially spliced transcript that retained the 7th intron appeared to accumulate more in *mtp5-1* than in wild type (Figure 4B), providing evidence that the *mtp5-1* splice site mutation at the 3′ end of intron 7 (Figure 1C) affects not only the position, but also the efficiency of *MTP5* transcript splicing.
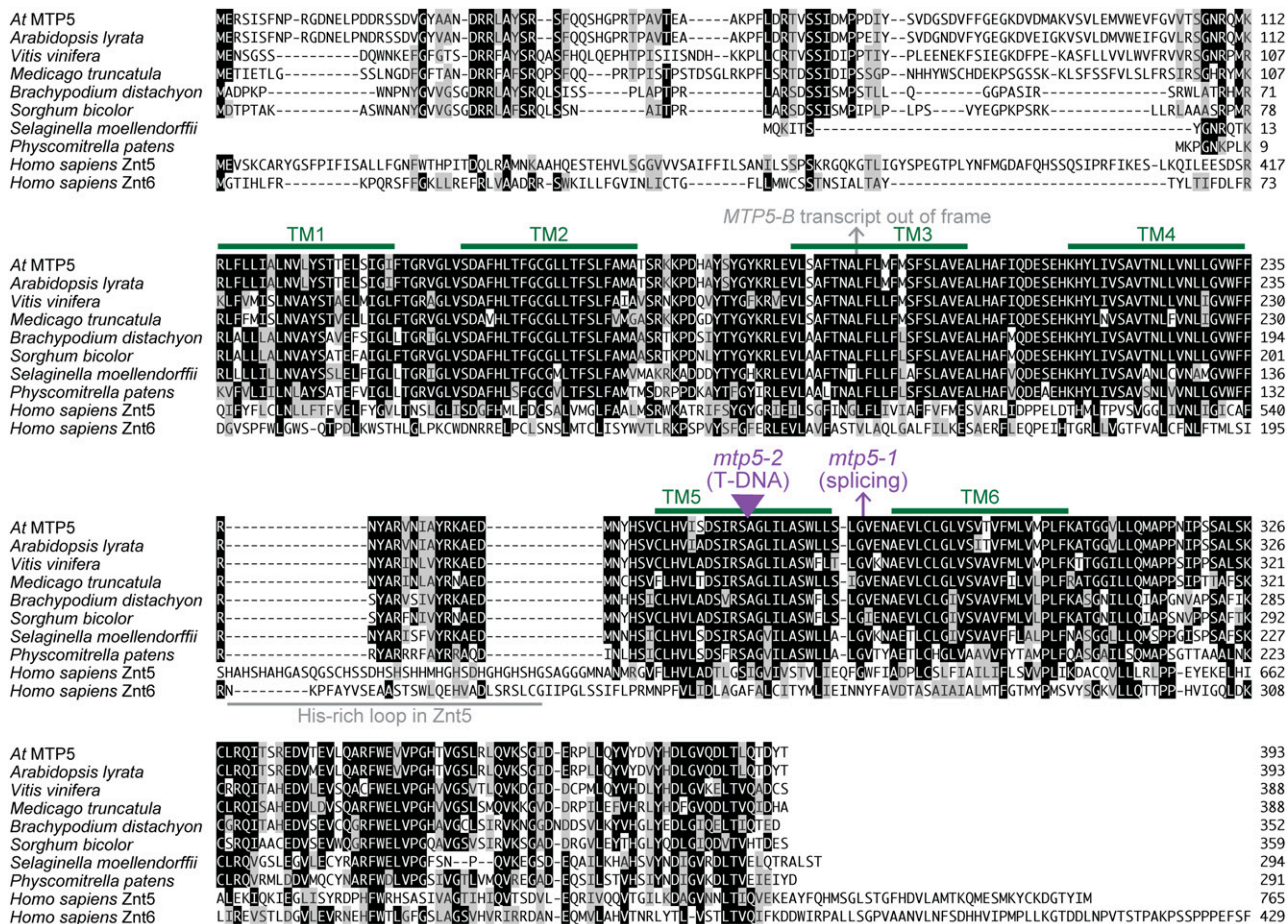
Figure 2 Alignment of *Arabidopsis* MTP5 and related proteins. *Arabidopsis thaliana* MTP5 (At3g12100; AAT44130.1) was aligned with likely orthologs from other plants (*Arabidopsis lyrata* XP_002884882.1, *Vitis vinifera* XP_002279787.1, *Medicago truncatula* XP_003625268.1, *Sorghum bicolor* XP_002453105.1, *Brachypodium distachyon* XP_003570736.1, *Selaginella moellendorffii* XP_002982633.1, *Physcomitrella patens* XP_001755969.1) and the human ZnT5 (*Homo sapiens* NP_075053.2; residues 296-765 of 765 residues) and ZnT6 (*Homo sapiens* NP_001180442; residues 1-429 of 501 residues) zinc transporters using the MegAlign program (DNASTAR) using the Clustal W method. Residues identical in at least five sequences are shaded in black boxes; chemically similar residues in at least five sequences are shaded in gray boxes. Potential transmembrane (TM) domains in *Arabidopsis thaliana* MTP5 predicted with Aramemnon (Schwacke *et al.* 2003) are marked with green lines; the His-rich loop found in Znt5 but not MTP5 orthologs is marked by a gray line. The position of the alternative splicing events that would lead to an out-of-frame sequence followed by premature termination codons caused by the *mtp5-1* mutation or detected in wild-type mRNA (the *MTP5-B* transcript) are indicated by arrows. The position of the *mtp5-2* T-DNA disruption is indicated with a triangle.

In addition to the inefficient splicing of *MTP5* introns 6 and 7, we found that intron 3 was alternatively spliced in both wild type and *mtp5* mutants. We detected two fully spliced *MTP5* transcripts, *MTP5-A* and *MTP5-B*, in 7-d-old seedlings; *MTP5-A* was more abundant than *MTP5-B* (Figure 4C). These transcripts used different 3′ splice sites of the third intron (Figure 4C); the *MTP5-B* transcript would truncate the encoded protein in the third predicted transmembrane domain (Figure 2). Because the stop codon in *MTP5-B* is at a position prior to the *mtp5-1* mutation in intron 7, we concluded that it is the *MTP5-A* transcript that is defective in *mtp5-1*.

Characterization of a second *mtp5* allele

To confirm that the mutation that we identified in *mtp5-1* caused the observed suppression of the IAA-conjugate resistance of *iar1*, we compared phenotypes of our original *mtp5-1* splicing allele and the *mtp5-2* T-DNA insertion allele. We crossed *mtp5-2* to the *iar1-3* mutant to determine whether this allele also restored IAA-conjugate sensitivity to *iar1*. Indeed, *iar1-3 mtp5-2* seedlings were significantly more sensitive to IAA-amino acid conjugates than *iar1-3* (Figure 3A), confirming that the *mtp5-1* splice-site mutation is a loss-of-function allele and that reducing MTP5 function can compensate for the lack of IAR1 activity in an *iar1* mutant. Unlike *mtp5-1* (Figure 3A and 5B), *mtp5-2* in an otherwise wild-type background was not significantly hypersensitive to IAA conjugates (Figure 3A).

Because MTP5 is a metal transporter homolog, we examined *mtp5* sensitivity to various metals in root growth inhibition assays. Unlike the *ilr3-1* mutant, which is specifically resistant to Mn^{2+} (Rampey *et al.* 2006), both *mtp5-1* and *mtp5-2* (in the wild-type *IAR1* background) displayed responses similar to wild type to all of the metals tested, including Mn^{2+}, Zn^{2+}, Co^{2+}, and Cd^{2+} (Figure 5A). Moreover, we found that driving expression of the *MTP5-A* cDNA in wild-type Col-0 seedlings behind the strong CaMV 35S promoter did not alter seedling root lengths on medium supplemented with one of several metals, including Mn^{2+}, Zn^{2+}, Co^{2+}, and Cd^{2+} (data not shown).

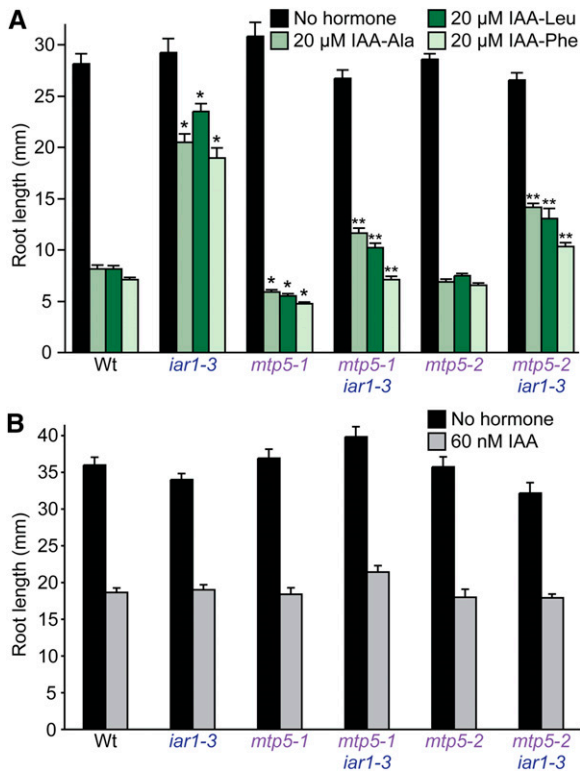**Figure 3** (A) *mtp5* mutations restore IAA-conjugate sensitivity to *iar1* roots. Col-0 (Wt), *iar1-3*, *mtp5-1*, *mtp5-2*, *mtp5-1 iar1-3*, and *mtp5-2 iar1-3* seedlings were grown on unsupplemented medium or medium containing 20 μM IAA-Ala, IAA-Leu, or IAA-Phe. (B) Like *iar1*, *mtp5*, and *mtp5 iar1* mutants respond normally to IAA. Seedlings listed in (A) were grown on unsupplemented medium or medium containing 60 nM IAA. Seedlings were grown in constant light under yellow filters for 8 (A) or 9 (B) d at 22°. Error bars indicate standard errors of the mean root lengths (n = 12). Single asterisks indicate single mutant root lengths significantly different from Wt; double asterisks indicate double mutant root lengths significantly different from *iar1-3* (two-tailed *t*-tests; $P < 0.001$).

mtp5-1 does not suppress other IAA-conjugate sensitivity mutants

To determine whether *mtp5-1* could suppress the IAA-conjugate resistance of mutants in addition to *iar1*, we constructed double mutants of *mtp5-1* with other IAA-conjugate resistant mutants, including the IAA-amino acid conjugate amidohydrolase mutants *iar3-1* (Davies *et al.* 1999) and *ilr1-5* (Rampey *et al.* 2006), which are resistant to the inhibitory effects of IAA conjugates that are substrates of the mutated hydrolases. For example, *iar3* is resistant to IAA-Ala and not IAA-Leu and IAR3 cleaves IAA-Ala more efficiently than IAA-Leu *in vitro* (Davies *et al.* 1999), whereas *ilr1* is resistant to IAA-Leu and not IAA-Ala and ILR1 cleaves IAA-Leu more efficiently than IAA-Ala *in vitro* (Bartel and Fink 1995). We examined root lengths of each double mutant after growth on IAA-amino acid conjugates. We found that *mtp5-1* failed to restore *ilr1-5* sensitivity to IAA-Leu or *iar3-1* sensitivity to IAA-Ala, and that the heightened sensitivity of *mtp5-1* to IAA-Leu was retained in the *iar3-1 mtp5-1* double mutant (Figure 5B). This lack of suppression of the amidohydrolase mutants establishes that *mtp5-1* is not a general suppressor of all conjugate response mutants. Moreover, the epistatic relationship of these mutants demonstrates that the increased IAA-conjugate sensitivity of the *mtp5-1* mutant requires intact conjugate hydrolases with specificity for the indicated IAA-amino acid.
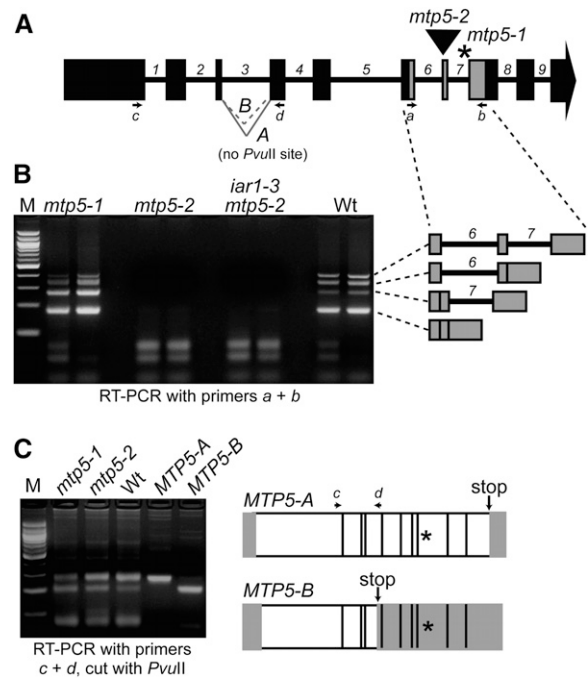

Figure 4 Alternative splicing of *MTP5* transcripts. (A) Model of *MTP5* gene showing exons (boxes), introns (numbered), positions of *mtp5* mutations (asterisk, *mtp5-1*; triangle, *mtp5-2*), primers used for RT-PCR amplification (arrows a-d), and the A and B *MTP5* splice variants of intron 3. (B) *mtp5-2* seedlings lack intact *MTP5* transcript, and *mtp5-1* and wild-type seedlings inefficiently splice *MTP5* introns 6 and 7. *MTP5* transcripts were detected via RT-PCR amplification using gene-specific primers (A and B) flanking both *mtp5* mutations with RNA isolated from 7-d-old *mtp5-1*, *mtp5-2*, *iar1-3 mtp5-2*, and Col-0 (Wt) seedlings. Adjacent lanes show PCR-amplification products of cDNA from two independent reverse transcription reactions using the same RNA. The identities of the four amplicons from the RT-PCR analysis using primers a and b were determined by sequencing and are shown to the right in gray. (C) *mtp5-1* and wild-type seedlings alternatively splice *MTP5* intron 3. Using gene-specific primers c and d (A), *MTP5* transcripts were amplified from cDNA reverse-transcribed from Col-0 (Wt), *mtp5-1*, and *mtp5-2* RNA. RT-PCR analysis revealed two transcripts in wild type and the two mutant alleles, designated *MTP5-A* and *MTP5-B*. Digesting the PCR products with *Pvu*II distinguished *MTP5-A*, which lacks a *Pvu*II site, from *MTP5-B*, which includes a *Pvu*II site (agarose gel image in C). Cloned *MTP5-A* and *MTP5-B* cDNAs were included as positive controls. The transcripts were differently spliced at the 3′ end of the third intron, resulting in a premature stop codon (arrows) in *MTP5-B*. Asterisks mark the position of the *mtp5-1* mutation. White boxes indicate the open reading frame of the resultant transcripts, and gray boxes show predicted untranslated regions.

DISCUSSION

Plant cation diffusion facilitator (CDF) transporters

We isolated an extragenic suppressor of the IAA-conjugate response mutant *iar1* and found that the defective gene encodes MTP5, a previously uncharacterized member of the CDF transporter family found in bacteria, yeast, animals, and plants. Plant CDF proteins usually have six predicted transmembrane domains (Figure 2) flanked by an N-terminal signature sequence and a C-terminal cation efflux domain (Mäser *et al.* 2001). There are 12 members of this family in *Arabidopsis*. Phylogenetic analysis and substrate specificity of characterized members separates the CDF family into three groups: Mn-CDF, Fe/Zn-CDF, and Zn-CDF (Montanini *et al.* 2007; Gustin *et al.* 2011). MTP5 is in the
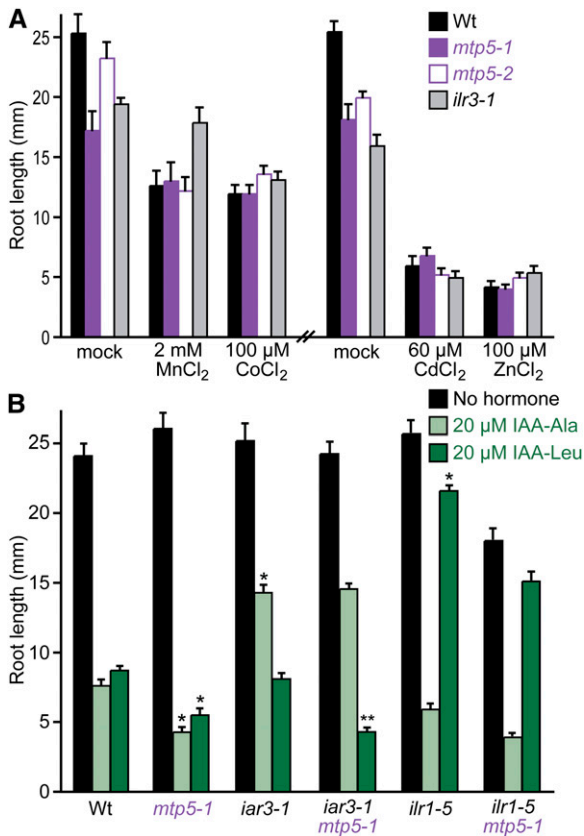
Figure 5 *mtp5* mutations do not alter metal sensitivity or restore IAA-amino acid sensitivity to IAA-conjugate hydrolase mutants. (A) *mtp5* mutant roots respond normally to inhibitory concentrations of various metals. Col-0 (Wt), *mtp5-1*, *mtp5-2*, and *ilr3-1* seedlings were grown on unsupplemented medium or medium containing 2 mM MnCl₂, 100 µM CoCl₂, 60 µM CdCl₂, or 100 µM ZnSO₄ in constant light under yellow filters for 8 d at 22°. Error bars indicate standard errors of the mean root lengths (n ≥ 9). (B) *mtp5-1* does not suppress the IAA-conjugate resistance of mutants defective in IAA-amino acid hydrolases. Col-0 (Wt), *iar3-1*, *ilr1-5*, *mtp5-1*, *iar3-1 mtp5-1*, and *mtp5-1 ilr1-5* seedlings were grown on unsupplemented medium or medium containing 20 µM IAA-Ala or IAA-Leu in constant light under yellow filters for 8 d at 22°. Error bars indicate SE of the mean root lengths (n ≥ 9). Single asterisks indicate single mutant root lengths significantly different from Wt; double asterisks indicate *iar3-1 mtp5-1* double mutant root lengths significantly different from *iar1-3* (two-tailed t-tests; P < 0.001). Significance was not calculated for *ilr1-5 mtp5-1* differences because the double mutant roots were shorter than the single mutant roots on unsupplemented medium.

Zn-CDF family; all biochemically-characterized members of this subfamily transport at least zinc (Montanini *et al.* 2007).

Although none are functionally characterized, MTP5 has apparent orthologs in a variety of plants, including *Medicago*, *Brachypodium*, *Sorghum*, *Selaginella*, and *Physcomitrella* (Figure 2), suggesting an early emergence of MTP5 during the evolution of land plants. These proteins are between 63 and 73% identical to *A. thaliana* and *A. lyrata* MTP5, which are 96% identical to each other. Less similarity is present in the region N-terminal to the first predicted transmembrane domain, which is missing in the MTP5 orthologs from *Selaginella* and *Physcomitrella*. The plant MTP5 homologs lack the His-rich loop found between transmembrane domains four and five in some zinc transporters, such as human ZnT5 (Figure 2) and *Arabidopsis* MTP1 and MTP3 (Kawachi *et al.* 2012).

Of the 12 *Arabidopsis* MTP (CDF) proteins, six are in the Zn-CDF subfamily (Montanini *et al.* 2007; Gustin *et al.* 2011). This subfamily includes the first characterized plant MTP protein, *Arabidopsis* ZAT (Van Der Zaal *et al.* 1999), now designated MTP1 (Mäser *et al.* 2001). MTP1 transports Zn²⁺ when heterologously expressed in *E. coli* proteoliposomes (Bloß *et al.* 2002), *mtp1* mutant roots accumulate less Zn²⁺ in vacuolar-like organelles (Kawachi *et al.* 2009), and transgenic plants overexpressing *MTP1* hyperaccumulate Zn²⁺ and have decreased Zn²⁺ sensitivity (Van Der Zaal *et al.* 1999). In contrast, we found no alterations in Zn²⁺ sensitivity when MTP5 was mutated or overexpressed.

Characterized AtMTP1 homologs in other plant species all are proposed to sequester metals in intracellular compartments or catalyze metal efflux from cells. For example, the *Thalspi caerulescens* (Tc) *ZTP1* gene is induced when soil is enriched with Zn²⁺, Cd²⁺, or Pb²⁺ (Assuncao *et al.* 2001). Heterologous expression of an AtMTP1 homolog from the tropical legume *Stylosanthes hamata*, ShMTP1, confers Mn²⁺ tolerance to yeast and *Arabidopsis* (Delhaize *et al.* 2003). ShMTP1-GFP fusions localize to plant tonoplasts and the yeast ER (Delhaize *et al.* 2003). Similarly, heterologous expression of PtdMTP1 from poplar (*Populus trichocarpa x P. deltoids*) confers Zn²⁺ resistance to yeast and *Arabidopsis*, and PtdMTP1-GFP fusions are vacuolar in both yeast and *Arabidopsis* (Blaudez *et al.* 2003). Interestingly, the *Thalspi goesingense* TgMTP1 gene gives rise to three transcript variants, *TgMTP1a*, *TgMTP1b*, and *TgMTP1c* (Kim *et al.* 2004). Expression of *TgMTP1a* in yeast confers resistance to Cd²⁺, Co²⁺, and Zn²⁺, whereas *TgMTP1b* expression confers resistance to Ni²⁺ (Persans *et al.* 2001). TgMTP1b localizes to the plasma membrane of *Arabidopsis* leaf protoplasts and may efflux Zn²⁺ from cells (Kim *et al.* 2004). Although we also found evidence for alternative splicing of *Arabidopsis* MTP5 (Figure 4), only one of these splice products (*MTP5-A*) is likely to encode an intact transporter.

Several MTP1 proteins have been tested for complementation of the yeast mutant *cot1 zrc1*, which is defective in vacuolar metal efflux (MacDiarmid *et al.* 2000). The three TgMTP1 isoforms, TcZTP1, *Thaspi arvense* MTP1, *Thaspi montanum var. fendleri* MTP1, *Arabidopsis lyrata* MTP1, AtMTP1, and PtdMTP1 all confer Zn²⁺ resistance when expressed in yeast (Blaudez *et al.* 2003; Kim *et al.* 2004). However, the authors of a previous study found that AtMTP1 did not complement the *cot1 zrc1* mutant (Bloß *et al.* 2002). Expression of TgMTPb truncations containing the N-terminus, C-terminus, the putative metal-binding His-rich domain, or various combinations of these domains do not complement the *cot1 zrc1* mutant, suggesting that the Zn²⁺ resistance that accompanies *TgMTPb* overexpression is related to transport and not due to binding excess Zn²⁺ by the His-rich domain. We transformed the *MTP5* cDNA driven by the glyceraldehyde-3-phosphate dehydrogenase constitutive promoter into wild-type and *cot1* and *zrc1* single and double mutant yeast lines but did not observe changes in relative growth in the presence of Zn²⁺ or Co²⁺ (data not shown). It is possible that *Arabidopsis* MTP5 does not function in yeast membranes. Alternatively, because the localization and identity of metals potentially transported by MTP5 are not known, this lack of complementation may be due to differences in location or metal specificity among MTP5 and the yeast Cot1p and Zrc1p proteins.

An *Arabidopsis* cation diffusion facilitator protein mutant

Beyond the suppression of the IAA-conjugate resistance of *iar1*, *mtp5-1*, and *mtp5-2* plants resembled wild type as seedlings and

adults (Figures 3 and 5 and data not shown). The *mtp5* mutants resembled wild type on media containing metals under all conditions tested (Figure 5A). In contrast, *mtp1* mutants have increased Zn^{2+} sensitivity (Kobae *et al.* 2004; Kawachi *et al.* 2009), and *mtp11* mutants (defective in a member of the Mn-CDF family) are more sensitive to Mn^{2+} (Delhaize *et al.* 2007; Peiter *et al.* 2007). RNAi lines silencing *MTP1* or *MTP3* also show Zn^{2+} hypersensitivity (Desbrosses-Fonrouge *et al.* 2005; Arrivault *et al.* 2006). It is possible that other transporters partially compensate for any loss of transport activity in the *mtp5* mutants. In this case, the *mtp5* mutation may modify subcellular metal concentration(s) adequately to compensate for the presumed transport defect in *iar1* seedlings, but not alter levels enough to cause toxic metal accumulation that would increase sensitivity to exogenous metals.

A working model for *mtp5* suppression of *iar1*

In eukaryotes, Zn^{2+} transport into or out of the cytosol occurs through the opposing action of two protein families, the ZIPs and CDFs (Kambe *et al.* 2004, 2006). ZIP proteins transport Zn^{2+} from outside cells and from intracellular compartments into the cytosol. In an opposing manner, CDFs transport Zn^{2+} out of the cytosol and into extracellular space or intracellular compartments. Homology thus suggests that the MTP5 CDF protein effluxes metals out of cells or into a subcellular compartment, whereas the IAR1 ZIP protein is predicted to move metals into cells or out of a subcellular compartment.

The mutant phenotypes and predicted protein functions suggest that MTP5 and IAR1 transport metals in an antagonistic fashion to regulate metal homeostasis, which in turn influences IAA-amino acid conjugate hydrolysis by compartmentalized enzymes (Figure 6). Based on the membrane topology of IAR1 homologs, one possibility is that IAR1 transports metals inhibitory to IAA-amino acid hydrolase function out of the compartment in which the hydrolases reside (Figure 6A). This compartment is likely to be the ER, because the yeast IAR1 ortholog Yke4p is ER-localized (Kumánovics *et al.* 2006), the hydrolases contain predicted N-terminal signal sequences and C-terminal ER retention signals (Bartel and Fink 1995; Davies *et al.* 1999), and both IAR3 and ILR1 have been localized to the ER in proteomics experiments (Dunkley *et al.* 2006). Metals impact hydrolase activity; for example, the *in vitro* activities of the IAA-conjugate hydrolases are enhanced by Mn^{2+}, and ILR1 activity is inhibited by Zn^{2+} (LeClere *et al.* 2002). Moreover, the crystal structure of the *Arabidopsis* ILR1-like homolog ILL2 reveals a di-metal binding site in the hydrolase active site that is typical of the M20 metallopeptidases family (Bitto *et al.* 2009). The IAA-conjugate resistance of *iar1* may result from an aberrant accumulation of inhibitory metals in the hydrolase compartment, which decreases hydrolysis of and therefore sensitivity to IAA-amino acid conjugates (Figure 6B). If MTP5 transports inhibitory metals into the hydrolase-containing compartment, an *mtp5 iar1* mutant would no longer be IAA-conjugate resistant because inhibitory metals would not accumulate, thus restoring wild-type levels of IAA-conjugate hydrolysis (Figure 6C). This model is consistent with our observation that double mutants defective in both *MTP5* and the *ILR1* or *IAR3* hydrolase genes remain resistant to IAA-Leu or IAA-Ala (Figure 5B), respectively, indicating that MTP5 functions upstream of the hydrolases.

This compensatory model is consistent with the function of yeast transporters similar to IAR1 and MTP5. When yeast are grown in low zinc medium, the IAR1 ortholog Yke4p moves zinc from the secretory pathway into the cytosol (Kumánovics *et al.* 2006). Intriguingly, loss of Yke4 can compensate for the loss of the Msc2p (Kumánovics *et al.* 2006), a CDF protein in the MTP5 subfamily that transports zinc into the ER (Li and Kaplan 2001; Ellis *et al.* 2005).
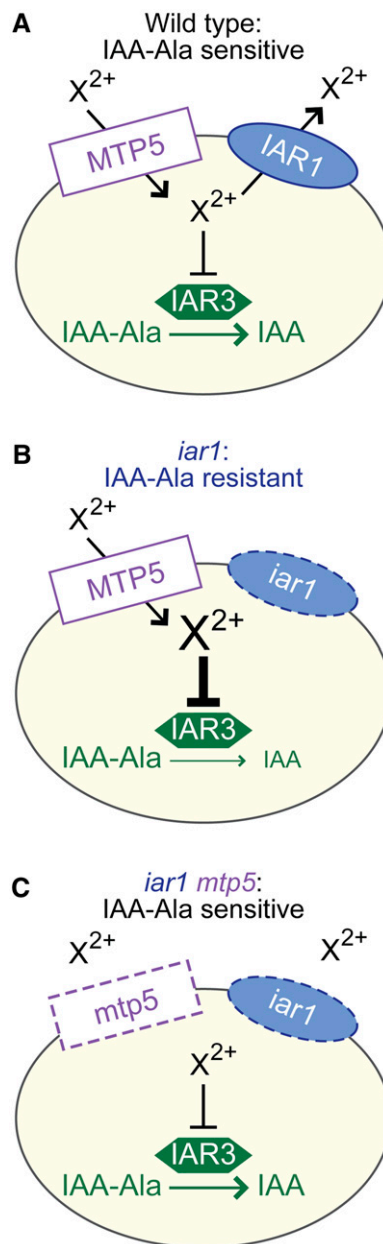
Figure 6 A working model for MTP5 and IAR1 function in IAA-conjugate responses in wild type (A), an *iar1* mutant (B), and an *iar1 mtp5* double mutant (C). The presence of IAA-amino acid hydrolases in the ER, the localization and function of MTP5 and IAR1 orthologs, and the *iar1* and *mtp5* mutant phenotypes (see text for details) suggest that MTP5 and IAR1 may transport Zn^{2+} or other metal(s) that inhibit hydrolase function into and out of, respectively, the ER. Validation or rejection of this model awaits localization of the MTP5 and IAR1 transporters and determination of their substrate specificities.

Whereas the model depicted in Figure 6 suggests that IAR1 and MTP5 occupy the same membrane, it is also possible that either or both MTP5 and IAR1 are located in a compartment that does not contain the hydrolases. When metal homeostasis is disrupted within this compartment, it may indirectly affect the metal environment of the ER, thus indirectly affecting IAA-conjugate hydrolysis. Distinguishing between these possibilities will be aided by characterization of the subcellular localizations and metal transport specificities of the

IAR1 and MTP5 proteins. Regardless of the subcellular localization of IAR1 and MTP5, however, it is clear that genetic studies of IAA-amino acid conjugate responsiveness are exquisitely sensitive to uncovering factors contributing to metal homeostasis. As this screen has not reached saturation, it is possible that continued studies will reveal additional components necessary to control the metal environment in which the hydrolases function.

Interestingly, CDF metal transporters may directly interact with a component from a signaling pathway to modify the binding partner's activity (Jirakulaporn and Muslin 2004). The C-terminal intracellular portions of mammalian Znt1 and worm CDF-1 bind the amino-terminal regulatory region of Raf-1, a protein kinase that regulates cell proliferation and differentiation (Jirakulaporn and Muslin 2004). Further, Raf-1 activity is dependent on Znt1 function, and *in vitro* binding does not occur upon addition of Zn^{2+} (Jirakulaporn and Muslin 2004). Some CDF transporters also form heterodimers, including yeast Msc2p and Zrg17p (Ellis *et al.* 2005) and the corresponding mammalian homologs ZnT5 and ZnT6 (Ellis *et al.* 2005; Fukunaka *et al.* 2009). Identification of *Arabidopsis* MTP5 binding partners may further elucidate the relationship between metal homeostasis and IAA-conjugate sensitivity.

LITERATURE CITED
Arrivault, S., T. Senger, and U. Kramer, 2006   The *Arabidopsis* metal tolerance protein AtMTP3 maintains metal homeostasis by mediating Zn exclusion from the shoot under Fe deficiency and Zn oversupply. Plant J. 46: 861–879.

Assuncao, A. G. L., P. D. Martins, S. De Folter, R. Vooijs, H. Schat *et al.*, 2001   Elevated expression of metal transporter genes in three accessions of the metal hyperaccumulator *Thlaspi caerulescens*. Plant Cell Environ. 24: 217–226.

Ausubel, F., R. Brent, R. E. Kingston, D. D. Moore, J. G. Seidman *et al.*, 1999   *Current Protocols in Molecular Biology*. Greene Publishing Associates and Wiley-Interscience, New York.

Bartel, B., and G. R. Fink, 1995   ILR1, an amidohydrolase that releases active indole-3-acetic acid from conjugates. Science 268: 1745–1748.

Bell, C. J., and J. R. Ecker, 1994   Assignment of 30 microsatellite loci to the linkage map of *Arabidopsis*. Genomics 19: 137–144.

Bitto, E., C. A. Bingman, L. Bittova, N. L. Houston, R. S. Boston *et al.*, 2009   X-ray structure of ILL2, an auxin-conjugate amidohydrolase from *Arabidopsis thaliana*. Proteins 74: 61–71.

Blaudez, D., A. Kohler, F. Martin, D. Sanders, and M. Chalot, 2003   Poplar metal tolerance protein 1 confers zinc tolerance and is an oligomeric vacuolar zinc transporter with an essential leucine zipper motif. Plant Cell 15: 2911–2928.

Bloß, T., S. Clemens, and D. H. Nies, 2002   Characterization of the ZAT1p zinc transporter from *Arabidopsis thaliana* in microbial model organisms and reconstituted proteoliposomes. Planta 214: 783–791.

Chang, H. C., and S. Lindquist, 1994   Conservation of Hsp90 macromolecular complexes in *Saccharomyces cerevisiae*. J. Biol. Chem. 269: 24983–24988.

Cheng, N. H., J. K. Pittman, B. J. Barkla, T. Shigaki, and K. D. Hirschi, 2003   The *Arabidopsis cax1* mutant exhibits impaired ion homeostasis, development, and hormonal responses and reveals interplay among vacuolar transporters. Plant Cell 15: 347–364.

Clemens, S., M. G. Palmgren, and U. Kramer, 2002   A long way ahead: understanding and engineering plant metal accumulation. Trends Plant Sci. 7: 309–315.

Clough, S. J., and A. F. Bent, 1998   Floral dip: a simplified method for *Agrobacterium*-mediated transformation of *Arabidopsis thaliana*. Plant J. 16: 735–743.

Davies, R. T., D. H. Goetz, J. Lasswell, M. N. Anderson, and B. Bartel, 1999   *IAR3* encodes an auxin conjugate hydrolase from *Arabidopsis*. Plant Cell 11: 365–376.

Delhaize, E., T. Kataoka, D. M. Hebb, R. G. White, and P. R. Ryan, 2003   Genes encoding proteins of the cation diffusion facilitator family that confer manganese tolerance. Plant Cell 15: 1131–1142.

Delhaize, E., B. D. Gruber, J. K. Pittman, R. G. White, H. Leung *et al.*, 2007   A role for the *AtMTP11* gene of *Arabidopsis* in manganese transport and tolerance. Plant J. 51: 198–210.

Desbrosses-Fonrouge, A. G., K. Voigt, A. Schroder, S. Arrivault, S. Thomine *et al.*, 2005   *Arabidopsis thaliana* MTP1 is a Zn transporter in the vacuolar membrane which mediates Zn detoxification and drives leaf Zn accumulation. FEBS Lett. 579: 4165–4174.

Dunkley, T. P., S. Hester, I. P. Shadforth, J. Runions, T. Weimar *et al.*, 2006   Mapping the Arabidopsis organelle proteome. Proc. Natl. Acad. Sci. USA 103: 6518–6523.

Eide, D. J., M. Broderius, J. Fett, and M. L. Guerinot, 1996   A novel iron-regulated metal transporter from plants identified by functional expression in yeast. Proc. Natl. Acad. Sci. USA 93: 5624–5628.

Ellis, C. D., C. W. MacDiarmid, and D. J. Eide, 2005   Heteromeric protein complexes mediate zinc transport into the secretory pathway of eukaryotic cells. J. Biol. Chem. 280: 28811–28818.

Fukunaka, A., T. Suzuki, Y. Kurokawa, T. Yamazaki, N. Fujiwara *et al.*, 2009   Demonstration and characterization of the heterodimerization of ZnT5 and ZnT6 in the early secretory pathway. J. Biol. Chem. 284: 30798–30806.

Gaither, L. A., and D. J. Eide, 2000   Functional expression of the human hZIP2 zinc transporter. J. Biol. Chem. 275: 5560–5564.

Gietz, R., and R. Schiestl, 1995   Transforming yeast with DNA. Methods Mol. Cell. Biol. 5: 255–269.

Gollhofer, J., C. Schlawicke, N. Jungnick, W. Schmidt, and T. J. Buckhout, 2011   Members of a small family of nodulin-like genes are regulated under iron deficiency in roots of *Arabidopsis thaliana*. Plant Physiol. Biochem. 49: 557–564.

Gustin, J. L., M. J. Zanis, and D. E. Salt, 2011   Structure and evolution of the plant cation diffusion facilitator family of ion transporters. BMC Evol. Biol. 11: 76.

Hall, J. L., and L. E. Williams, 2003   Transition metal transporters in plants. J. Exp. Bot. 54: 2601–2613.

Haughn, G. W., and C. Somerville, 1986   Sulfonylurea-resistant mutants of *Arabidopsis thaliana*. Mol. Gen. Genet. 204: 430–434.

Huang, L., C. P. Kirschke, Y. Zhang, and Y. Y. Yu, 2005   The *ZIP7* gene (*Slc39a7*) encodes a zinc transporter involved in zinc homeostasis of the Golgi apparatus. J. Biol. Chem. 280: 15456–15463.

Jirakulaporn, T., and A. J. Muslin, 2004   Cation diffusion facilitator proteins modulate Raf-1 activity. J. Biol. Chem. 279: 27807–27815.

Kambe, T., Y. Yamaguchi-Iwai, R. Sasaki, and M. Nagao, 2004   Overview of mammalian zinc transporters. Cell. Mol. Life Sci. 61: 49–68.

Kambe, T., T. Suzuki, M. Nagao, and Y. Yamaguchi-Iwai, 2006   Sequence similarity and functional relationship among eukaryotic ZIP and CDF transporters. Genomics Proteomics Bioinformatics 4: 1–9.

Kawachi, M., Y. Kobae, H. Mori, R. Tomioka, Y. Lee *et al.*, 2009   A mutant strain *Arabidopsis thaliana* that lacks vacuolar membrane zinc transporter MTP1 revealed the latent tolerance to excessive zinc. Plant Cell Physiol. 50: 1156–1170.

Kawachi, M., Y. Kobae, S. Kogawa, T. Mimura, U. Kramer *et al.*, 2012   Amino acid screening based on structural modeling identifies critical residues for the function, ion selectivity and structure of Arabidopsis MTP1. FEBS J. 279: 2339–2356.

Kim, D., J. L. Gustin, B. Lahner, M. W. Persans, D. Baek *et al.*, 2004   The plant CDF family member TgMTP1 from the Ni/Zn hyperaccumulator *Thlaspi goesingense* acts to enhance efflux of Zn at the plasma membrane when expressed in *Saccharomyces cerevisiae*. Plant J. 39: 237–251.

Kobae, Y., T. Uemura, M. H. Sato, M. Ohnishi, T. Mimura *et al.*, 2004 Zinc transporter of *Arabidopsis thaliana* AtMTP1 is localized to vacuolar membranes and implicated in metal homeostasis. Plant Cell Physiol. 45: 1749–1758.

Koncz, C., J. Schell, and G. P. Rédei, 1992 T-DNA transformation and insertion mutagenesis, pp. 224–273 in *Methods in Arabidopsis Research*, edited by C. Koncz, N.-H. Chua, and J. Schell. World Scientific, Singapore.

Kumánovics, A., K. E. Poruk, K. A. Osborn, D. M. Ward, and J. Kaplan, 2006 *YKE4* (YIL023C) encodes a bidirectional zinc transporter in the endoplasmic reticulum of *Saccharomyces cerevisiae*. J. Biol. Chem. 281: 22566–22574.

Lasswell, J., 2000 *Genetic Analyses of Auxin Metabolism and of the Transition to Flowering in the Model Plant Arabidopsis thaliana* Dept. of Biochemistry & Cell Biology, Rice University, Houston, TX.

Lasswell, J., L. E. Rogg, D. C. Nelson, C. Rongey, and B. Bartel, 2000 Cloning and characterization of *IAR1*, a gene required for auxin conjugate sensitivity in Arabidopsis. Plant Cell 12: 2395–2408.

Last, R. L., and G. R. Fink, 1988 Tryptophan-requiring mutants of the plant *Arabidopsis thaliana*. Science 240: 305–310.

LeClere, S., and B. Bartel, 2001 A library of *Arabidopsis* 35S-cDNA lines for identifying novel mutants. Plant Mol. Biol. 46: 695–703.

LeClere, S., R. Tellez, R. A. Rampey, S. P. T. Matsuda, and B. Bartel, 2002 Characterization of a family of IAA-amino acid conjugate hydrolases from *Arabidopsis*. J. Biol. Chem. 277: 20446–20452.

Li, L., and J. Kaplan, 2001 The yeast gene *MSC2*, a member of the cation diffusion facilitator family, affects the cellular distribution of zinc. J. Biol. Chem. 276: 5036–5043.

Li, X., S. Chanroj, Z. Wu, S. M. Romanowsky, J. F. Harper *et al.*, 2008 A distinct endosomal Ca2+/Mn2+ pump affects root growth through the secretory process. Plant Physiol. 147: 1675–1689.

MacDiarmid, C. W., L. A. Gaither, and D. J. Eide, 2000 Zinc transporters that regulate vacuolar zinc storage in *Saccharomyces cerevisiae*. EMBO J. 19: 2845–2855.

Magidin, M., J. K. Pittman, K. D. Hirschi, and B. Bartel, 2003 *ILR2*, a novel gene regulating IAA conjugate sensitivity and metal transport in *Arabidopsis thaliana*. Plant J. 35: 523–534.

Marschner, H., 1995 *Mineral Nutrition of Higher Plants*. Academic Press, San Diego.

Mäser, P., S. Thomine, J. I. Schroeder, J. M. Ward, K. Hirschi *et al.*, 2001 Phylogenetic relationships within cation-transporter families of *Arabidopsis thaliana*. Plant Physiol. 126: 1646–1667.

Michaels, S. D., and R. M. Amasino, 1998 A robust method for detecting single-nucleotide changes as polymorphic markers by PCR. Plant J. 14: 381–385.

Montanini, B., D. Blaudez, S. Jeandroz, D. Sanders, and M. Chalot, 2007 Phylogenetic and functional analysis of the Cation Diffusion Facilitator (CDF) family: improved signature and prediction of substrate specificity. BMC Genomics 8: 107.

Neff, M. M., J. D. Neff, J. Chory, and A. E. Pepper, 1998 dCAPS, a simple technique for the genetic analysis of single nucleotide polymorphisms: experimental applications in *Arabidopsis thaliana* genetics. Plant J. 14: 387–392.

Normanly, J., P. Grisafi, G. R. Fink, and B. Bartel, 1997 Arabidopsis mutants resistant to the auxin effects of indole-3-acetonitrile are defective in the nitrilase encoded by the NIT1 gene. Plant Cell 9: 1781–1790.

Peiter, E., B. Montanini, A. Gobert, P. Pedas, S. Husted *et al.*, 2007 A secretory pathway-localized cation diffusion facilitator confers plant manganese tolerance. Proc. Natl. Acad. Sci. USA 104: 8532–8537.

Persans, M. W., K. Nieman, and D. E. Salt, 2001 Functional activity and role of cation-efflux family members in Ni hyperaccumulation in *Thlaspi goesingense*. Proc. Natl. Acad. Sci. USA 98: 9995–10000.

Rampey, R. A., S. Leclere, M. Kowalczyk, K. Ljung, G. Sandberg *et al.*, 2004 A family of auxin-conjugate hydrolases that contributes to free indole-3-acetic acid levels during Arabidopsis germination. Plant Physiol. 135: 978–988.

Rampey, R. A., A. W. Woodward, B. N. Hobbs, M. P. Tierney, B. Lahner *et al.*, 2006 An *Arabidopsis* basic helix-loop-helix leucine zipper protein modulates metal homeostasis and auxin conjugate responsiveness. Genetics 174: 1841–1857.

Rosso, M. G., Y. Li, N. Strizhov, B. Reiss, K. Dekker *et al.*, 2003 An *Arabidopsis thaliana* T-DNA mutagenized population (GABI-Kat) for flanking sequence tag-based reverse genetics. Plant Mol. Biol. 53: 247–259.

Schwacke, R., A. Schneider, E. Van Der Graaff, K. Fischer, E. Catoni *et al.*, 2003 ARAMEMNON, a novel database for *Arabidopsis* integral membrane proteins. Plant Physiol. 131: 16–26.

Stasinopoulos, T. C., and R. P. Hangarter, 1990 Preventing photochemistry in culture media by long-pass light filters alters growth of cultured tissues. Plant Physiol. 93: 1365–1369.

Strader, L. C., and B. Bartel, 2011 Transport and metabolism of the endogenous auxin precursor indole-3-butyric acid. Mol Plant 4: 477–486.

Taylor, K. M., and R. I. Nicholson, 2003 The LZT proteins; the LIV-1 subfamily of zinc transporters. Biochim. Biophys. Acta 1611: 16–30.

Van Der Zaal, B. J., L. W. Neuteboom, J. E. Pinas, A. N. Chardonnens, H. Schat *et al.*, 1999 Overexpression of a novel *Arabidopsis* gene related to putative zinc-transporter genes from animals can lead to enhanced zinc resistance and accumulation. Plant Physiol. 119: 1047–1055.

Winter, D., B. Vinegar, H. Nahal, R. Ammar, G. V. Wilson *et al.*, 2007 An "Electronic Fluorescent Pictograph" browser for exploring and analyzing large-scale biological data sets. PLoS ONE 2: e718.

Woodward, A. W., and B. Bartel, 2005 Auxin: regulation, action, and interaction. Ann. Bot. (Lond.) 95: 707–735.

Communicating editor: M. Estelle